

Thermal expansivity of mantle relevant magnesium silicates derived from vibrational spectroscopy at high pressure

ANASTASIA CHOPELAS*

Max Planck Institut für Chemie, Postfach 3060, 55020 Mainz, Germany

ABSTRACT

Thermal expansivities for the MgSiO_3 phases of orthoenstatite, high clinoenstatite, ilmenite, and majorite; and for stishovite were estimated using the thermodynamic Maxwell relation $(\partial S/\partial P)_T = -(\partial V/\partial T)_P$, where the entropies at high pressures were derived using a statistical method and spectroscopic data. The spectroscopically determined thermal expansivities for all minerals are in excellent agreement with previously determined volumetric data, where available. A value of $3.25(10) \times 10^{-5} \text{ K}^{-1}$ for orthoenstatite at room temperature was obtained; this value is situated in the middle of the large spread of reported values and is in excellent agreement with the two latest volumetric determinations. For high clinoenstatite, α at room T is estimated as $2.56(9) \times 10^{-5} \text{ K}^{-1}$. This method provides good high temperature estimates of α for the high-pressure polymorphs, where data are scanty or unavailable. Included in this report are previous data for the Mg_2SiO_4 phases and MgO for completeness. The following equations may be used to extrapolate α to higher temperatures at 1 atm in 10^{-5} K^{-1} : $\alpha(\text{majorite}) = 2.95 + 0.000521x$; $\alpha(\gamma\text{-Mg}_2\text{SiO}_4) = 2.70 + 0.000648x$; $\alpha(\text{ilmenite}) = 2.64 + 0.000537x$; $\alpha(\text{perovskite}) = 2.51 + 0.000805x$; and $\alpha(\text{stishovite}) = 2.19 + 0.000485x$, where x is $(T/\text{K}-750)$.

INTRODUCTION

The topic “thermal expansivity” brought Orson Anderson and myself together during my early years in Mainz and lead to our collaborative work then and many fruitful exchanges in the ensuing years. It is my pleasure to be able to contribute this comprehensive article covering thermal expansivity of all mantle relevant magnesium silicates to a volume honoring Orson.

Thermal expansivity α of mantle minerals is of fundamental importance to physical and compositional models of the Earth in several ways. First, its knowledge allows for a more precise assessment of in situ mineral densities for comparison to seismic models. Accurate values at ambient conditions are important because these are used as a basis for extrapolation to mantle conditions. Secondly, dynamical models of the Earth are affected dramatically by the value of thermal expansivity especially at the bottom of the mantle. For example, a large decrease in α with depth narrows the calculated diameter of plumes or upwellings, more in line with the observations. Third, α is required to convert lateral velocity anomalies to lateral

thermal anomalies. And last, α is required for calculating the adiabatic gradient of the Earth.

The value for α of the Earth relevant magnesium silicates is extremely small and its accurate measurement by volumetric methods tests the resolution limits of most equipment. The most common method for determining thermal expansivity is the X-ray determination of the lattice parameters vs. temperature. Powder diffractometry of the minerals of interest tends to be further complicated by the low symmetry of these materials. Reports of α even for common and abundant surface minerals such as MgSiO_3 enstatite may vary by over a factor of two as shown in the present work. Measurement of the even less compressible metastable deeper Earth phases at high temperatures and ambient conditions is even more of a challenge. Only scanty and incomplete data exist for the MgSiO_3 phases of majorite, high clinopyroxene, and ilmenite; and for stishovite.

I previously showed (Chopelas 1996) that thermal expansivity may be well constrained by using information obtained from vibrational spectroscopy at high pressure. The advantage of this method is that the measurements are performed at room temperature and the frequencies vs. pressure are very precisely determined. In all cases, several measurements were taken within the stability field of the phase. The pressure dependence of the vibrational frequencies did not change. The variation of frequency with pressure provides a basis for estimating entropy vs. pressure, which directly yields thermal expansivity through the Maxwell relation

*Current Address: Department of Physics, 4505 Maryland Parkway, Box 454002, Las Vegas, Nevada 89154-4002, U.S.A.
E-mail: chopelas@physics.unlv.edu

$$\left(\frac{\partial V}{\partial T}\right)_P = -\left(\frac{\partial S}{\partial P}\right)_T \quad (1)$$

where S is entropy, V is volume, P is pressure, and T is temperature. Thermal expansivity is then

$$\alpha = \frac{1}{V} \left(\frac{\partial V}{\partial T}\right)_P \quad (2)$$

To calculate α from the variation of entropy vs. pressure, the molar volume of the phase must be known at the pressure and temperature of interest. At 1 atm, the calculation of volume at higher temperatures is obtained by using the present expansivity results as temperature is increased. Note that the variation in $\partial S/\partial P$ greatly exceeds the variation in volume, thus the uncertainty in volume does not contribute significantly to the uncertainty in the resulting expansivity. At higher pressures, the bulk moduli and their pressure derivatives for each of the phases are used to calculate volumes at various pressures. Even though there are some variations in these values for the higher pressure polymorphs in the literature, the variations in the calculated volumes using the different elasticity values are much smaller than the uncertainties in $\partial S/\partial P$ obtained from the spectroscopic results. And again the volume uncertainty does not contribute significantly to the expansivity uncertainty. The most important parameter here is an accurate computation of the entropy rather than the volume.

For minerals in which no significant configurational entropy has been observed, as the ones in this study, the relationship of vibrational frequencies to thermal expansivity may be clearly seen by comparing expansivity to heat capacity. For pyrope (Suzuki and Anderson 1983), these two functions vs. temperature are identical in shape (Fig. 1). This is not a general relationship and may not be applied to many simple fourfold-coordinated compounds such as Si, Ge, or diamond, where negative expansivities are found at very low temperatures. The relationship of heat capacity to expansivity as shown in Figure 1 becomes clearer when the physical consequences

of raising the temperature of a mineral are considered. At room temperature, the normal modes or vibrations of a crystal lattice at or below about 300 cm^{-1} are predominantly active in the crystal. This can be seen in the anti-Stokes spectrum where the modes above 300 cm^{-1} have almost no intensity. As the temperature is increased, more of the higher frequency normal modes become activated; as seen by the intensity increase of the higher energy modes with increasing temperature in the anti-Stokes spectrum. This means more energy can be absorbed, meaning an increased heat capacity and its expansion is thus increased per unit temperature because more bonds (modes) become active in the expansion.

In my previous work (Chopelas 1996), thermal expansivity from spectroscopic data for MgO and $\gamma\text{-Mg}_2\text{SiO}_4$ was shown to closely match those measured volumetrically over a large temperature range at 1 atm. Furthermore, for MgO, the Anderson-Grüneisen parameter (Anderson 1967), $\delta_T = (\partial \ln \alpha / \partial \ln V)_T$, derived from the spectroscopic method exactly matched that found from $\delta_T = -(1/\alpha K_T)(\partial K_T / \partial T)_P$, where K_T is the isothermal bulk modulus, at all temperatures (Isaak et al. 1989). The spectroscopic method was then applied to MgSiO_3 perovskite where previously reported volumetric measurements varied significantly from one another. The spectroscopic results were consistent with the previous volumetric (lower) values measured by two laboratories, published in three different reports (Funamori and Yagi 1993; Utsumi et al. 1995; Wang et al. 1994). The spectroscopic method also provided valuable constraints for δ_T and γ_{th} , the thermal Grüneisen parameter, for perovskite.

In this report, I extend the application of the spectroscopic method for determining thermal expansivity to the remaining magnesium silicates relevant to the Earth's mantle, including MgSiO_3 orthoenstatite, high clinoenstatite, majorite, ilmenite, and SiO_2 stishovite. For completeness, I include the previous results for magnesium silicates. The thermal Grüneisen parameter $\gamma_{\text{th}} = \alpha K_T V / C_V$, where C_V is the constant volume heat capacity, is also constrained for these minerals. The present α estimates for orthoenstatite provides an independent assessment in order to sort out the extreme variation in previously reported volumetric data. Moreover, determination of α for metastable high clinoenstatite and remaining high pressure magnesium silicates yield values in good agreement with the scant available data and consistent with the other thermoelastic parameters for these materials. The present estimates provide a good basis for extrapolation of α to mantle temperatures for these minerals.

METHODOLOGY

Using the following equations to obtain entropy at various pressures and temperatures requires that a reasonable density of states be constructed whose spectrum and pressure dependency represents that observed experimentally. This can be obtained by careful enumeration of the modes using symmetry analysis, factor group analysis, and mode assignments based on cation or isotopic substitution, high pressure as well as variable temperature measurements of the vibrational modes. This has been done previously for all the minerals under examination here; their vibrational models are provided in the appendix for completeness.

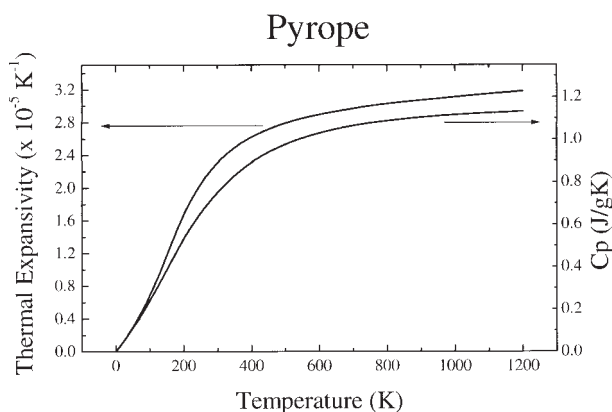


FIGURE 1. Comparison of the temperature dependence of the thermal expansivity (upper curve, left axis) to that for the constant pressure heat capacity, C_p , (lower curve, right axis). Data are obtained from the article by (Suzuki and Anderson 1983).

For all minerals, the procedure for estimating entropy is the same. The constant volume heat capacity C_V is estimated from

$$C_V = 3 N k \int_0^\infty \frac{e^x}{(e^x - 1)^2} x^2 g(v) dv \quad (3)$$

where N is the number of atoms in the unit cell, k Boltzmann's constant, v the frequency of vibration, x is $h\nu/kT$, h Planck's constant, and $g(v)$ the density of states. Then C_V is converted to the constant pressure heat capacity, C_P , using the anharmonic correction of

$$C_P = C_V + T V \alpha^2 K_T \quad (4)$$

which may also be expressed as $C_V(1+\alpha\gamma T)$. The "anharmonic" correction " $\alpha\gamma T$ " is very small until about 700 K. By 1000 K, it is about 5% of the total value of the heat capacity, most of which is due to the contribution from T . At high temperatures, γ and α vary little with pressure and temperature (Anderson et al. 1992). As mentioned later, α is solved by iteration.

TABLE 1. Comparison of the weighted average of the spectroscopic mode Grüneisen parameters from $\alpha = \sum C_i \gamma_i / \sum C_i$ to the thermal Grüneisen parameter $\gamma_{th} = \alpha K_T / V C_V$

Mineral	$\langle \gamma \rangle$	γ_{th}
Forsterite	1.19	1.29
β -MgSiO ₃	1.29	1.39
γ -MgSiO ₃	1.10	1.25
MgO	1.47	1.52
Stishovite	1.40	1.34
MgSiO ₃ Orthoenstatite	1.20	1.28
MgSiO ₃ High Clinoen	1.09	1.22
MgSiO ₃ Majorite	1.32	1.28
MgSiO ₃ Ilmenite	1.24	1.22
MgSiO ₃ Perovskite	1.43	1.42

Notes Parameters for all minerals for calculation are found in Tables 2 and 3. a = Chopelas (1990), b = Chopelas (1991), c = Chopelas (1994), d = Chopelas (1996), e = this study using α at room T determined in this study

TABLE 2. Thermoelastic parameters for the minerals listed in Table 1

Mineral	V_0 (cm ³ /mol)	K_T (GPa)	K'_0	C_V (J/mol·K)
Forsterite	43.62	128 ^b	4.4 ^c	116.4
β -MgSiO ₃	40.51 ^f	173 ^g	4.2 ^h	113.2
γ -MgSiO ₃	39.53	183 ⁱ	5.0	112.1
MgO	11.25	161 ^j	4.1 ^k	36.7 ^l
Stishovite	14.02	303 ^m	2.8 ⁿ	41.4
MgSiO ₃ Orthoen.	31.32	103	10.8	80.6
MgSiO ₃ High Cen.	30.43	123 ^o	5.6 ^p	79.4
MgSiO ₃ Majorite	28.58 ^q	160 ^r	4.5 ^s	79.9
MgSiO ₃ Ilmenite	26.35	210 ^a	4 ^{bb}	77.4 ^{aa}
MgSiO ₃ Perovskite	24.44	263 ^c	4 ^{bb}	81.9 ^{dd}

Notes a = Isaak et al. (1991), b = Li et al. (1996), c = Robie et al. (1978), d = Horiuchi and Sawamoto (1981), e = Sawamoto et al. (1984), f = Chopelas (1991), g = Akaogi et al. (1989), h = Fisher et al. (1984), i = Rigden and Jackson (1991), j = Chopelas et al. (1994), k = e.g., Isaak et al. (1989), l = Jackson and Niesler (1982), m = Robie et al. (1978), n = Hill et al. (1983), o = Ross et al. (1990), p = Hofmeister (1996), q = Ohashi (1984), r = Flesch et al. (1998), s = Zhao et al. (1995), t = Krupka et al. (1985a), u = Krupka et al. (1985b), v = Angel et al. (1992), w = Jones and Angel (1994), x = Chopelas (1999), y = Angel et al. (1989), z = Yagi et al. (1992), aa = Yusa et al. (1993), ab = Yamada (1982), ac = Veidner and Ito (1985), ad = Ashida et al. (1988), ae = Assumed but fit the compressibility data with the K_T , cc = Widner et al. (1993), dd = Akaogi and Ito (1993).

TABLE 3. Comparison of spectroscopically determined thermal expansivity to those derived from volume measurements in 10⁻⁶K⁻¹

Mineral	Spectroscopic	Volumetric
Forsterite	2.40 ^b	2.72 ^c
β -MgSiO ₃	1.89 ^b	2.01 ^c
γ -MgSiO ₃	1.84 ^b	1.86 ^c
MgO	2.79 ^b	3.11 ^e
Stishovite	1.33(8) ^b	14.2 ^c
MgSiO ₃ Orthoen.	3.25(10) ^b	2.2–4.77 ^c
MgSiO ₃ High Cen.	2.59(10) ^b	Not measured
MgSiO ₃ Majorite	2.24(9) ^b	2.36 ^c
MgSiO ₃ Ilmenite	1.7(1) ^b	k
MgSiO ₃ Perovskite	1.8(1) ^b	1.72 ^c

Notes a = Chopelas (1996), b = Kajiyoshi (1986), c = Suzuki et al. (1980), d = Suzuki et al. (1979), e = Isaak et al. (1989), f = this work, g = Fei et al. (1990), h = Ito et al. (1974a), i = Ito et al. (1974b), j = Table 3, k = pyrope data from Suzuki and Anderson (1983), l = only averaged value between 298 and 876 K of 2.440^g K⁻¹ reported by Ashida et al. (1988), m = Funamori and Yagi (1993), n = Utsumi et al. (1995), o = Yagi et al. (1994).

The soundness of the vibrational models checked for consistency by (1) the comparison of calorimetric data to those obtained using Equations 3 and 4, as done previously for all materials, and (2) comparison of the spectroscopically derived weighted average Grüneisen parameter $\langle \gamma \rangle = \sum C_i \gamma_i / \sum C_i$, where C_i is the Einstein heat capacity and γ_i the mode Grüneisen parameter of mode i , to γ_{th} obtained as above. As seen in Table 1 for all minerals, all $\langle \gamma \rangle$ values are very near or match γ_{th} well within the experimental uncertainties for the required parameters (found in Tables 2 and 3). For the MgSiO₃ high pressure phases of high clinoenstatite, majorite, and ilmenite, this study provides an α value at room T so γ_{th} may be calculated.

To obtain entropy, the following equation is integrated over temperature

$$\Delta S = \int_0^T \frac{C_P}{T} dT \quad (5)$$

where T_i is the temperature of interest. The entropy values are calculated at various pressures to find $S(P)$. Since α is used to calculate C_P , the results from Equation 2 are substituted back into Equation 4. The process is continued by successive iteration until convergence occurs.

To estimate entropy at higher pressures, the frequencies in the vibrational models (Appendix Tables 1–9) are shifted in accordance with measurements of $v(P)$, as represented by the mode Grüneisen parameters $\gamma_i = (K_T/V_0)(\partial v/\partial P)_T$ assigned to each frequency range. Fundamentally the resulting value of a second order polynomial for use in Equations 1 and 2. In absence of high temperature measurements of $v(P)$, $S(P)$ at high temperature is obtained by varying T in Equations 3 to 5, which is the quasi-harmonic approach. This method yields excellent results for most minerals. It may be surprising that the small frequency drop due to temperature does not need to be included in these calculations for accurate results, but this results in a small biasing of the entropy results which cancels when the pressure dependence of the entropy is computed. The quasi

harmonic approach is less successful for the low pressure polymorphs of Mg_2SiO_4 (forsterite and $\beta\text{-Mg}_2\text{SiO}_4$) and of MgSiO_3 (the pyroxenes). For these materials, thermal expansivity is slightly underestimated at high temperatures, very likely due to the widely differing compressibilities of the two polyhedra, MgO_6 octahedra and SiO_4 tetrahedra, in these materials. This leads to a gap in the vibrational spectrum, where all the high energy modes are associated with the very incompressible SiO_4 tetrahedra and have very low mode γ_i values. The underestimation of α at high temperatures suggests that as the higher energy vibrations become active, the pressure shifts of these modes will increase and likewise increase the estimated expansivity. Actual measurement of the mode pressure dependencies at the higher temperatures is thus required to accurately estimate α at

higher temperatures. In contrast, the high energy modes of the high pressure polymorphs are intercoupled and are thus not separable into independent contributions from various polyhedral units. For the high-pressure polymorphs, thermal expansivities at high temperatures are in exact accord with previous volumetric measurements as seen in the following sections.

THERMAL EXPANSIVITY RESULTS

Consistency checks

In general, the thermal expansivity is inversely proportional to the bulk modulus, which is fairly reasonable considering that γ_{th} and V/C_V vary little among the minerals, Tables 1 and 2. A graph of α vs. K_T at room temperature shows this clearly (Fig. 2). All points except MgO and $\text{Mg}_2\text{Al}_2\text{O}_4$ in the figure follow a fairly narrow trend even though the structures and compositions of these materials vary significantly. So, it is reasonable to expect that very incompressible minerals such as stishovite will have the lowest α values whereas the more compressible minerals such as orthoenstatite will have one of the highest α values at room temperature. This correlation is corroborated by the following results for the minerals.

Orthoenstatite

The value for α at room temperature reported in the literature over the years has varied by more than a factor of two, despite it being a common and important rock forming mineral (Table 4). Recently, two careful and thorough measurements of α on end-member MgSiO_3 Pbca orthoenstatite yielded room temperature values about in the middle of this range at 3.1 to $3.2 \times 10^{-5} \text{ K}^{-1}$ (Hugh-Jones 1997; Zhao et al. 1995). The present α estimate of $3.25(10) \times 10^{-5} \text{ K}^{-1}$ is in exact agreement with these recent volumetric measurements (Table 4), which also allows a more confident estimate for γ_{th} of 1.28 for this mineral.

Furthermore, the rapid decline in α with pressure with a reported δ_T of 11.8 (Zhao et al. 1995) is also corroborated by the spectroscopic results. The Raman results for orthoenstatite vs. pressure show a large decrease in the pressure shifts of all frequencies at 5 GPa (Chopelas 1999). Thus, the pressure shift for entropy also decreases significantly, yielding a thermal expansivity of $2.28 \times 10^{-5} \text{ K}^{-1}$ at 5 GPa, in accord with the previous volumetric results. The present results yield a δ_T of about 10, approximately equal to the high $K' = (dK/dP)$ of about 10 observed for this mineral (Hugh-Jones and Angel 1994; Webb and Jackson 1993; Zhao et al. 1995), which is consistent with the empirically determined approximation that $\delta_T \approx K'_0$ (Anderson et al. 1992).

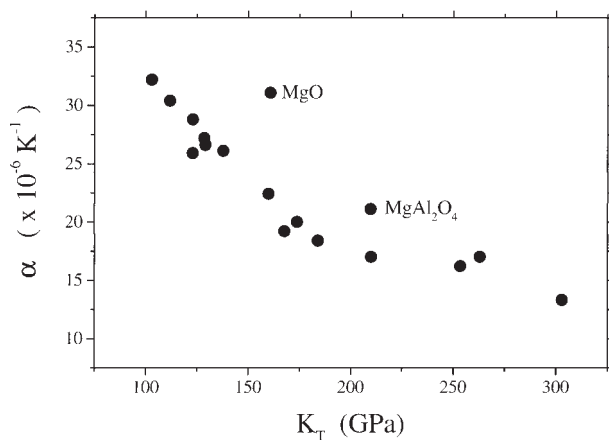


FIGURE 2. Plot of the volume thermal expansivity at room temperature vs. the isothermal bulk modulus for several minerals. Aside from those listed in Tables 2 and 3, values are also plotted for MgAl_2O_4 (198 GPa, $2.11 \times 10^{-5} \text{ K}^{-1}$), Al_2O_3 (254 GPa, $1.62 \times 10^{-5} \text{ K}^{-1}$), fayalite (138 GPa, $2.61 \times 10^{-5} \text{ K}^{-1}$), CaO (112 GPa, $3.04 \times 10^{-5} \text{ K}^{-1}$), pyrope (169 GPa, $2.36 \times 10^{-5} \text{ K}^{-1}$). The above data are in the article by Anderson et al. (1992).

TABLE 4. Thermal expansivity values for MgSiO_3 orthoenstatite reported in the literature in 10^{-5} K^{-1}

α	Source	α	Source
3.6	Sarver and Hummel (1962)	3.35	Yang and Ghose (1994)
2.4	Skinner (1966)	3.08	Zhao et al. (1995)
4.77	Frisillo and Buljan (1972)	3.22	Hugh-Jones (1997)
2.08	Dietrich and Arndt (1982)	3.25(10)	This work

TABLE 5. Temperature dependence of the thermal expansivity for magnesium silicates at $K_{\text{th}} = 10$

Temperature (K)	$\gamma\text{-MgSiO}_3$		Majorite		Pyrope		Ilmenite		Stishovite	
	Spectroscopic	Volumetric	Spectroscopic	Volumetric	Spectroscopic	Volumetric	Spectroscopic	Volumetric	Spectroscopic	Volumetric
300	1.84	1.86	2.24	2.36	1.75	2.44	1.36	1.43		
500	2.43	2.30	2.75	2.80	2.40	2.44	1.94	1.70		
700	2.68	2.45	2.89	2.97	2.61	2.44	2.17	1.97		
900	2.82	2.60	3.02	3.07	2.74	2.44	2.27	2.24		
1000	2.87	2.60	3.09	3.11	2.77		2.30	2.37		

Note Uncertainties are approximately $\pm 0.10^{-5} \text{ K}^{-1}$ for all spectroscopic estimates and shown on Figures 4 to 6. a = Suzuki et al. (1979), b = garnet composition 72.6% pyrope, 15.7% almandine, 4.3% andradite, 6.1% uvarovite, and 0.6% spessartine (Suzuki et al. 1983), c = Ashida et al. (1988), d = Fei et al. (1990); Ito et al. (1974a); Ito et al. (1974b), e = for example, Suzuki (1975), f = Yagi (1993) and Tsumi et al. (1995); Wang et al. (1994).

High clinoenstatite (C2/c)

High clinoenstatite is a metastable phase converting to low clinoenstatite at about 4 GPa upon pressure release even at room temperature (see figure in Chopelas and Boehler 1992a). The volumetric measurement of α at 1 atm is thus not possible. Here the frequencies are linearly extrapolated to 1 atm, reflected in the vibrational model in Appendix Table 2, before applying Equations 1 to 5. A previous estimate of α using a systematic crystal chemical approach and data for other clinopyroxenes is $3.25 \times 10^{-5} \text{ K}^{-1}$ (Zhao et al. unpublished data), similar to that for orthoenstatite above. Such a high value for α for high clinopyroxene is however unlikely because the pressure shifts of the frequencies are significantly lower than for orthoenstatite and the estimated bulk modulus is suggested to be near that of forsterite (Angel et al. 1992; Zhao et al. unpublished data) and higher than that of orthoenstatite. This leads us to expect that α for this polymorph must be lower than that of orthoenstatite and near that of forsterite. Indeed, the spectroscopic α estimate is $2.56(10) \times 10^{-5} \text{ K}^{-1}$ for high clinoenstatite at room temperature.

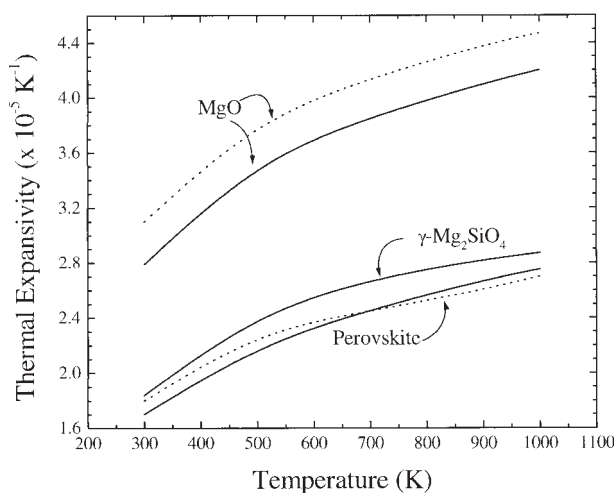


FIGURE 3. Plot of the spectroscopically estimated thermal expansivity vs. temperature at 1 atm (solid lines) compared with the volumetrically determined values (dotted lines) for MgO, MgSiO₃ perovskite, and γ -Mg₂SiO₄. The volumetrically determined values for γ -Mg₂SiO₄ are not plotted in the figure for clarity but examination of their values in Table 5 show that they are in accord with the present estimates plotted here. These values are from (Chopelas 1996).

TABLE 5—Continued

MgO		Perovskite	
Spectroscopic	Volumetric	Spectroscopic	Volumetric
2.79	3.10	1.8	1.70
3.54	3.84	2.3	2.20
3.86	4.14	2.45	2.46
4.10	4.38	2.6	2.67
4.20	4.47	2.7	2.75

For all the remaining minerals examined in this study, comparisons of the room temperature thermal expansivities estimated by the spectroscopic method to those by volumetric methods, where available, show excellent agreement (Table 3).

Majorite and Ilmenite

For the MgSiO₃ majorite and ilmenite phases, no atmospheric pressure volumetric measurements vs. temperature exist. That shown in Table 3 for majorite is the previously measured value for pyrope (Suzuki and Anderson 1983). For ilmenite, only an average α between 298 and 876 K of $2.44 \times 10^{-5} \text{ K}^{-1}$ has been reported (Ashida et al. 1988). It is expected that high tempera-

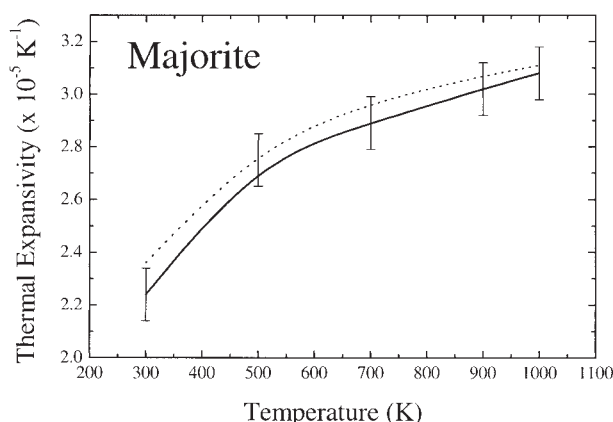


FIGURE 4. Comparison of the spectroscopically estimated thermal expansivity of MgSiO₃ majorite garnet vs. temperature at 1 atm (solid line) to the volumetrically determined values for pyrope garnet (dotted line) (Suzuki and Anderson 1983). The uncertainties for the spectroscopic values are shown in the figure.

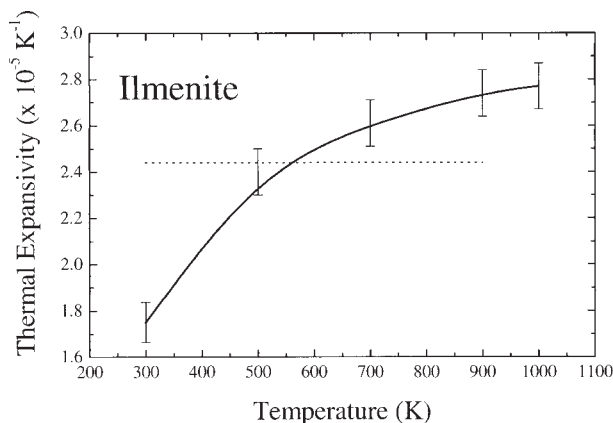


FIGURE 5. Comparison of the spectroscopically estimated thermal expansivity of MgSiO₃ ilmenite vs. temperature (solid line) to the volumetric determination averaged from 298 to 876 K (dotted line) (Ashida et al. 1988). The uncertainties for the spectroscopic values are shown in the figure.

ture estimates of α using the present method should be as successful as those for γ -Mg₂SiO₄, MgSiO₃ perovskite, and MgO (Chopelas 1996), shown in Figure 3 and Table 5, since these are also transition zone or lower mantle phases. Indeed, the results for majorite exactly match the previous pyrope results (Fig. 4 and Table 5), which is not surprising since pyrope and majorite have nearly the same bulk moduli, 169 GPa for the former (Suzuki and Anderson 1983) and 160 GPa for the latter (Yagi et al. 1992). For ilmenite, the high temperature results are consistent with the previous average value (Fig. 5 and Table 5). In both cases, the spectroscopic method provides a good basis for extrapolation of thermal expansivity to deep mantle conditions.

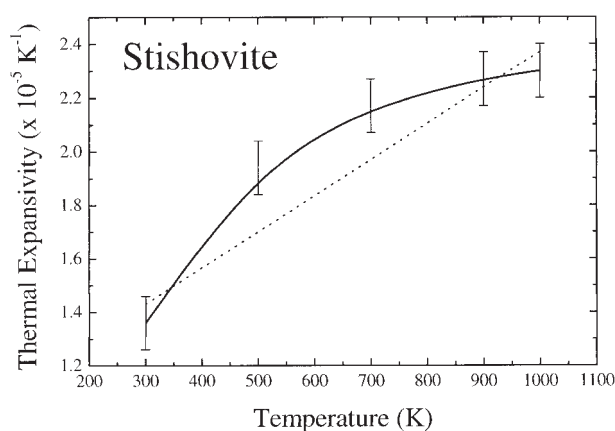


FIGURE 6. Comparison of the spectroscopically estimated thermal expansivity of stishovite vs. temperature (solid line) to the volumetric determination (dotted line) (Fei et al. 1990; Ito et al. 1974a; Ito et al. 1974b). The uncertainties for the spectroscopic values are shown in the figure.

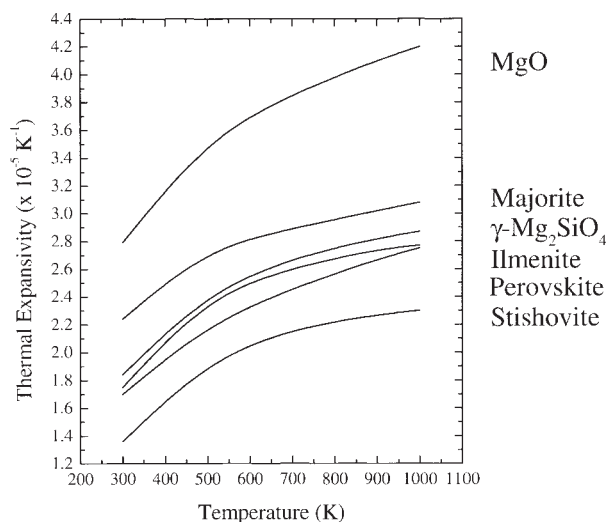


FIGURE 7. Comparison of the thermal expansivities vs. temperature from 300 to 1000 K for the minerals reported in this study. As bulk modulus increases, the thermal expansivity decreases.

TABLE 6. Parameters for extrapolation of thermal expansivity of the high pressure polymorphs to higher temperatures using $\alpha = \{A + B(T-750)\} \times 10^{-5} \text{ K}^{-1}$, where T is in K

Mineral	A	$B \times 10^6$
γ -Mg ₂ SiO ₄	2.70	0.648
MgSiQ majorite	2.85	0.521
MgSiQ ilmenite	2.64	0.537
MgSiQ perovskite	2.51	0.805
Stishovite	2.19	0.485

Stishovite

The α measured volumetrically for stishovite has been reported as a straight line function of $(1.02 + 0.00135 \cdot T/K) \times 10^{-5} \text{ K}^{-1}$, (Fei et al. 1990; Ito et al. 1974a; Ito et al. 1974b), shown in Figure 6. The present results are in excellent agreement with the former measurements but provides a more physically realistic function for accurate extrapolation to deep mantle temperatures.

Figure 7 summarizes and compares the results for the minerals in this study and shows that the present expansivities for these phases increase in value as the bulk modulus decreases.

EXTRAPOLATION OF α TO HIGH PRESSURES AND TEMPERATURES

For the above determinations of thermal expansivity for these mantle minerals to be useful for geophysical modeling, a simple relationship for extrapolation to higher temperatures and pressures is highly desirable. To extrapolate the 1 atm expansivities to higher temperatures, the slope of α vs. temperature above about 750 K is determined (Table 6). This simple relationship can then be further modified for pressure using (Chopelas and Boehler 1992b):

$$\alpha = \alpha_0 \left(\frac{V}{V_0} \right)^{\delta_T \frac{V}{V_0}} \quad (6)$$

Because all of these materials have similar K' values (Table 2), it is expected that all these materials will have similar values of δ_T (Anderson et al. 1992). For perovskite, a value of 5 for δ_T closely matched the high pressure behavior of α from 1 atm to 80 GPa at room temperature (Chopelas 1996). Other estimates for this parameter for perovskite also yield about 5 at room temperature and about 4 above the Debye temperature, for perovskite, about 1000 K (Anderson 1998). Thus, for parameterization in Earth models, a reasonable starting value for δ_T is 5 at room temperature and gradually reducing to 4 as the temperature rises to above 1000 K for all the materials listed in Table 6.

ACKNOWLEDGMENTS

I thank G. Serghiou for a critical reading of the text and Y. Zhao for helpful discussion. Useful reviews were provided by O.L. Anderson, L. Dubrovinsky, and S. Sinogeikin.

REFERENCES CITED

- Akaogi, M. and Ito, E. (1993) Heat capacity of MgSiO₃ perovskite. *Geophysical Research Letters*, 20, 105–108.
- Akaogi, M., Ito, E., and Navrotsky, A. (1989) Olivine- modified spinel- spinel transitions in the system Mg₂SiO₄-Fe₂SiO₄: Calorimetric measurements, thermochemical calculation, and geophysical application. *Journal of Geophysical Research*, 94, 15671–15685.
- Anderson, O.L. (1967) Equation for thermal expansivity in planetary interiors. *Journal*

- of Geophysical Research, 72, 3661–3668.
- (1998) Thermoelastic properties of MgSiO_3 perovskite using the Debye approach. *American Mineralogist*, 83, 23–35.
- Anderson, O.L., Isaak, D., and Oda, H. (1992) High-temperature elastic constant data on minerals relevant to geophysics. *Reviews of Geophysics*, 30, 57–92.
- Angel, R.J., Chopelas, A., and Ross, N.L. (1992) Stability of high-density clinoenstatite at upper-mantle pressures. *Nature*, 358, 322–324.
- Angel, R.J., Finger, L.W., Hazen, R.M., Kanzaki, M., Weidner, D.J., Liebermann, R.C., and Veblen, D.R. (1989) Structure and twinning of single-crystal MgSiO_3 garnet synthesized at 17 GPa and 1800 °C. *American Mineralogist*, 74, 509–512.
- Ashida, T., Kume, E., Ito, E., and Navrotsky, A. (1988) MgSiO_3 ilmenite: Heat capacity, thermal expansivity, and enthalpy of transformation. *Physics and Chemistry of Minerals*, 16, 239–245.
- Chopelas, A. (1990) Thermal properties of forsterite at mantle pressures derived from vibrational spectroscopy. *Physics and Chemistry of Minerals*, 17, 149–157.
- (1991) Thermal properties of $\beta\text{-Mg}_2\text{SiO}_4$ at mantle pressures derived from vibrational spectroscopy: Implications for the mantle at 400 km depth. *Journal of Geophysical Research*, 96, 11817–11829.
- (1996) Thermal expansivity of lower mantle phases MgO and MgSiO_3 perovskite at high pressure derived from vibrational spectroscopy. *Physics of the Earth and Planetary Interiors*, 98, 3–15.
- (1999) Estimates of mantle relevant Clapeyron slopes in the MgSiO_3 system from high pressure spectroscopic data. *American Mineralogist*, 84, 233–246.
- Chopelas, A. and Boehler, R. (1992a) Raman spectroscopy of high pressure MgSiO_3 phases synthesized in a CO_2 laser heated diamond anvil cell. In Y. Syono, and M. Manghnani, Eds., *High Pressure Research: Application to Earth and Planetary Science*, p. 101–108. Terra publishing, Tokyo.
- Chopelas, A. and Boehler, R. (1992b) Thermal expansivity in the lower mantle. *Geophysical Research Letters*, 19, 1983–1986.
- Chopelas, A., Boehler, R., and Ko, J. (1994) Thermodynamics and behavior of $\gamma\text{-Mg}_2\text{SiO}_4$ at high pressure: Implications for Mg_2SiO_4 phase equilibrium. *Physics and Chemistry of Minerals*, 21, 351–359.
- Dietrich, P. and Arndt, J. (1982) Effects of pressure and temperature on the physical behavior of mantle-relevant olivine, orthopyroxene, and garnet: I. Compressibility, thermal properties and macroscopic Grüneisen parameters. In W. Schreyer, Ed. *High-Pressure Research in Geosciences*, p. 209–306. Schweizerbart'sche Verlagsbuchhandlungen, Stuttgart.
- Fei, Y., Saxena, S.K., and Navrotsky, A. (1990) Internally consistent thermodynamic data and equilibrium phase relations for compounds in the system MgO-SiO_2 at high pressure and high temperature. *Journal of Geophysical Research*, 95, 6915–6928.
- Flesch, L.M., Li, B., and Liebermann, R.C. (1998) Sound velocities of polycrystalline MgSiO_3 -orthopyroxene to 10 GPa at room temperature. *American Mineralogist*, 83, 444–451.
- Frisillo, A.L. and Buljan, S.T. (1972) Linear thermal expansion coefficients of orthopyroxene to 1000 °C. *Journal of Geophysical Research*, 77, 7115–7117.
- Funamori, N. and Yagi, T. (1993) High pressure and high temperature *in situ* x-ray observation of MgSiO_3 perovskite under lower mantle conditions. *Geophysical Research Letters*, 20, 387–390.
- Hill, R.J., Newton, M.D., and Gibbs, G.V. (1983) A crystal chemical study of stishovite. *Journal of Solid State Chemistry*, 47, 185–200.
- Hofmeister, A.M. (1996) Thermodynamic properties of stishovite at mantle conditions determined from pressure variations of vibrational modes. In M.D. Dyr, C. McCammon, and M.W. Schaefer, Eds., *Mineral Spectroscopy: A Tribute to Roger G. Burns*, p. 215–227. The Geochemical Society, Houston.
- Hofmeister, A.M. and Ito, E. (1992) Thermodynamic properties of MgSiO_3 ilmenite from vibrational spectra. *Physics and Chemistry of Minerals*, 18, 423–432.
- Horiuchi, H. and Sawamoto, H. (1981) $\beta\text{-Mg}_2\text{SiO}_4$: Single-crystal X ray diffraction study. *American Mineralogist*, 66, 568–575.
- Hugh-Jones, D. (1997) Thermal expansion of MgSiO_3 and FeSiO_3 ortho- and clinopyroxenes. *American Mineralogist*, 82, 689–696.
- Hugh-Jones, D.A. and Angel, R.J. (1994) A compressional study of MgSiO_3 orthoenstatite up to 8.5 GPa. *American Mineralogist*, 79, 405–410.
- Isaak, D.G., Anderson, O.L., and Goto, T. (1989) Measured elastic modulus of single-crystal MgO up to 1800 K. *Physics and Chemistry of Minerals*, 16, 703–714.
- (1991) Elasticity of single crystal forsterite measured to 1700 K. *Journal of Geophysical Research*, 95, 5895–5906.
- Ito, E. and Yamada, H. (1982) Stability relations of silicate spinels, ilmenites, and perovskites. In S. Akimoto, and M.H. Manghnani, Eds., *High Pressure Research in Geophysics*, p. 405–419. Center for Academic Publishing of Japan, Tokyo.
- Ito, E., Kawada, K., and Akimoto, S. (1974a) Thermal expansion of stishovite. *Physics of the Earth and Planetary Interiors*, 8, 277–281.
- (1974b) Erratum. *Physics of the Earth and Planetary Interiors*, 9, 371.
- Jackson, I. and Niesler, H. (1982) The elasticity of periclase to 3 GPa and some geophysical implications. In S. Akimoto, and M.H. Manghnani, Eds., *High Pressure Research in Geophysics*, p. 98–113. Center of Academic Publications of Japan, Tokyo.
- Kajiyoshi, K. (1986) High temperature equation of state for mantle minerals and their anharmonic properties. Okayama University, Okayama, Japan.
- Krupka, K.M., Hemingway, B.S., Robie, R.A., and Kerrick, D.M. (1985a) High-temperature heat capacities and derived thermodynamic properties of anthophyllite, diopside, dolomite, enstatite, bronzite, talc, tremolite, and wollastonite. *American Mineralogist*, 70, 261–271.
- Krupka, K.M., Robie, R.A., Hemingway, B.S., Kerrick, D.M., and Ito, J. (1985b) Low-temperature heat capacities and derived thermodynamic properties of anthophyllite, diopside, enstatite, bronzite, and wollastonite. *American Mineralogist*, 70, 249–260.
- Li, B., Gwanmesia, G.D., and Liebermann, R.C. (1996) Sound velocities of olivine and beta polymorphs of Mg_2SiO_4 at Earth's transition zone pressures. *Geophysical Research Letters*, 23, 2259–2262.
- Ohashi, Y. (1984) Polysynthetically-twinned structures of enstatite and wollastonite. *Physics and Chemistry of Minerals*, 10, 217–229.
- Rigden, S.M. and Jackson, I. (1991) Elasticity of germanate and silicate spinels at high pressure. *Journal of Geophysical Research*, 96, 9999–10006.
- Robie, R.A., Hemingway, B.S., and Fisher, J.R. (1978) Thermodynamic properties of minerals and related substances at 298.15 K and 1 bar pressure and higher temperature. *Geological Survey Bulletin* 1452.
- Robie, R.A., Hemingway, B.S., and Takai, M. (1982) Heat capacities and entropies of Mg_2SiO_4 , Mn_2SiO_4 , and Co_2SiO_4 between 5 and 380 K. *American Mineralogist*, 67, 470–482.
- Ross, N.L., Shu, J.-F., Hazen, R.M., and Gasparik, T. (1990) High-pressure crystal chemistry of stishovite. *American Mineralogist*, 75, 739–747.
- Sarver, J.F. and Hummel, F.A. (1962) Stability relations of magnesium metasilicate pyroxenes. *Journal of the American Ceramic Society*, 45, 152–157.
- Sawamoto, H., Weidner, D.J., Sasaki, S., and Kumazawa, M. (1984) Single crystal elastic properties of the modified spinel (beta) phase of Mg_2SiO_4 . *Science*, 224, 749–751.
- Skinner, B.J. (1966) Thermal expansion. In S.P. Clark Jr., Ed. *Handbook of Physical Constants*, p. 76–95. Geological Society of America, Boulder, Colorado.
- Suzuki, I. (1975) Thermal expansion of periclase and olivine and their anharmonic properties. *Journal of Physics of the Earth*, 23, 145–159.
- Suzuki, I. and Anderson, O. (1983) Elasticity and thermal expansion of a natural garnet up to 1000 K. *Journal of Physics of the Earth*, 31, 125–138.
- Suzuki, I., Ohtani, E., and Kumazawa, M. (1979) Thermal expansion of $\gamma\text{-Mg}_2\text{SiO}_4$. *Journal of the Physics of the Earth*, 27, 53–61.
- (1980) Thermal expansion of modified spinel, $\beta\text{-Mg}_2\text{SiO}_4$. *Journal of the Physics of the Earth*, 28, 273–280.
- Utsumi, W., Funamori, N., Yagi, T., Ito, E., Kikegawa, T., and Shimomura, O. (1995) Thermal expansivity of MgSiO_3 perovskite under high pressures up to 20 GPa. *Geophysical Research Letters*, 22, 1005–1008.
- Wang, Y., Weidner, D.J., Liebermann, R.C., and Zhao, Y. (1994) P-V-T equation of state of $(\text{Mg,Fe})\text{SiO}_3$ perovskite: constraints on composition of the lower mantle. *Physics of the Earth and Planetary Interiors*, 83, 13–40.
- Webb, S.L. and Jackson, I. (1993) The pressure dependence of the elastic moduli of single-crystal orthopyroxene ($\text{Mg}_{0.8}\text{Fe}_{0.2}\text{SiO}_3$). *European Journal of Mineralogy*, 5, 1111–1119.
- Weidner, D.J. and Ito, E. (1985) Elasticity of MgSiO_3 in the ilmenite phase. *Physics of the Earth and Planetary Interiors*, 40, 65–70.
- Weidner, D.J., Sawamoto, H., Sasaki, S., and Kumazawa, M. (1984) Single crystal elastic properties of the spinel phase of Mg_2SiO_4 . *Journal of Geophysical Research*, 89, 7852–7860.
- Weidner, D.J., Wang, Y., and Yeganeh-Haeri, A. (1993) Equation of state properties of mantle perovskites (abstract). *EOS Transactions of the American Geophysical Union*, 74, 571.
- Yagi, T., Uchiyama, Y., Akaogi, M., and Ito, E. (1992) Isothermal compression curve of MgSiO_3 tetragonal garnet. *Physics of the Earth and Planetary Interiors*, 74, 1–7.
- Yang, H. and Ghose, S. (1994) Thermal expansion, Debye temperature and Grüneisen parameter of synthetic $(\text{Fe, Mg})\text{SiO}_3$ orthopyroxenes. *Physics and Chemistry of Minerals*, 20, 575–586.
- Yusa, H., Akaogi, M., and Ito, E. (1993) Calorimetric study of MgSiO_3 garnet and pyroxene: Heat capacities, transition enthalpies, and equilibrium phase relations in MgSiO_3 at high pressures and temperatures. *Journal of Geophysical Research*, 98, 6453–6460.
- Zhao, Y., Schiffler, D., and Shankland, T.J. (1995) High P-T single-crystal x-ray diffraction study of thermoelasticity of MgSiO_3 orthopyroxene. *Physics and Chemistry of Minerals*, 22, 393–398.

MANUSCRIPT RECEIVED APRIL 8, 1999

MANUSCRIPT ACCEPTED OCTOBER 6, 1999

PAPER HANDLED BY DONALD ISAAC

APPENDIX

Vibrational models for magnesium silicates in this study. The first three modes in each of the models represents the acoustic modes. The remainder are optic mode continua. Einstein oscillators are assigned very narrow frequency ranges to facilitate the calculations at high pressures. The mode Grüneisen parameters, γ_i , are used to obtain the pressure shifts of the frequency ranges using the bulk moduli listed in Table 2. Tables A1 through A5 are from Chopelas (1999).

APPENDIX TABLE 1. Pbcu Orthoenstatite

Lower limit	Upper limit	Number of modes	γ_i
0	65	1	0.2
0	67	1	0.3
0	110	1	1.23
83	90	3	2.32
110	120	3	3.26
120	140	5	3.3
140	168	10	1.46
168	223	12	1.75
223	245	12	1.23
245	323	28	1.25
323	350	12	1.93
350	362	12	1.1
380	390	8	1.1
398	447	32	0.7
516	553	20	0.7
580	630	16	0.6
656	752	16	0.63
853	903	12	0.36
886	937	16	0.55
1014	1035	20	0.62

APPENDIX TABLE 2. C2/c Clinoenstatite

Lower limit	Upper limit	Number of modes	γ_i
0	95	1	0.80
0	104	1	0.80
0	172	1	2.4
120	155	2	1.10
165	484	6	1.7
216	280	2	0.90
229	416	11	1.4
380	577	20	0.64
680	682	2	0.57
714	716	2	0.46
829	831	5	0.43
1005	1007	4	0.54
1023	1026	3	0.62

APPENDIX TABLE 3. I4/a Majorite

Lower limit	Upper limit	Number of modes	γ_i
0	70	1	0.75
0	70	1	0.75
0	140	1	1.3
136	400	60	1.42
350	400	36	1.305
195	400	33	1.305
458	723	60	0.86
803	1081	48	0.86

APPENDIX TABLE 4. $R\bar{3}$ Ilmenite

Lower limit	Upper limit	Number of modes	γ_i
0	168.7	1	0.75
0	184.5	1	0.75
0	301.3	1	1.3
287	337	2	1.6
337	595	13	1.35
595	700	10	1.1
735	799	2	1.1

APPENDIX TABLE 5. P6mm Perovskite

Lower limit	Upper limit	Number of modes	γ_i
0	130	1	0.85
0	150	1	0.85
0	223	1	2.5
240	335	12	1.8
335	440	12	1.1
440	540	15	0.95
590	680	9	0.75
700	780	7	0.75
890	891	2	0.75

APPENDIX TABLE 6. P6mm Forsterite

Lower limit	Upper limit	Number of modes	γ_i
0	98	1	1.1
0	99	1	1.1
0	171	1	1.6
105	145	2	1.2
170	227	7	0.92
240	385	12	1.45
280	410	12	1.35
305	470	12	1.4
405	505	8	0.6
505	644	12	0.63
838	839	4	0.49
868	869	3	0.46
916	917	4	0.38
975	976	5	0.66

From Chopelas (1990).

APPENDIX TABLE 7. Imma β -MgSiQ

Lower limit	Upper limit	Number of modes	γ_i
0	118	1	0.95
0	118	1	0.95
0	198	1	1.45
86	140	1	1.65
140	185	2	1.6
185	232	3	1.5
232	340	8	1.35
250	330	6	0.9
360	505	12	0.85
340	485	4	1.65
350	520	12	1.4
430	580	4	1.1
505	645	11	0.82
530	580	2	1.35
710	711	2	0.83
795	796	2	1.1
810	930	8	0.82
965	966	2	0.85
1020	1021	2	0.85

From Chopelas (1991).

Appendix continued on next page

APPENDIX TABLE 8. Fd3m γ -MgSiQ

Lower limit	Upper limit	Number of modes	γ_i
0	138	1	0.5
0	155	1	0.5
0	253	1	1.08
280	325	3	1.5
320	580	12	1.2
360	390	6	1.3
372	480	4	0.99
545	620	6	0.66
785	796	6	1.26
834	835	2	0.93

Note: From Chopelas et al. (1994).

APPENDIX TABLE 9. P4 γ Stishovite

Lower limit	Upper limit	Number of modes	γ_i
0	186	1	1.3
0	227	1	1.3
0	405	1	1.7
190	470	2	0.7
470	585	3	1.6
580	700	3	2.3
836	1020	2	1.03
725	950	1	0.7
588	590	2	1.32
753	755	1	1.26
965	967	1	1.21

Note: Slightly modified version of that presented in Hofmeister and Ito (1992).